A PERMANENT MAGNET SYNCHRONOUS WIND GENERATOR FOR VEHICULAR APPLICATION

Saeed Masoumi KAZRAJI, Saheb KHANABDAL, Mohammad Hosein HOLAKOOIE, Mohammad Bagher Bannae SHARIFIAN

Department of Electrical and Computer Engineering University of Tabriz, Tabriz, Iran
s.masoumi90@ms.tabrizu.ac.ir, s.khanabdal90@ms.tabrizu.ac.ir, hosein.holakooie@gmail.com, sharifian@tabrizu.ac.ir

Abstract: *A driver for a brushless dc motor (BLDCM) which is supplied by a wind generator (WG) is proposed in this paper. The proposed system uses a buck converter with high efficiency and control unit for implementation maximum power point tracking (MPPT) technique. No optimal characteristic of the WG or an anemometer for wind speed measuring is needed while the WG works is variable speed mode, whereas simplicity and reliability of the proposed system is improved, cost and mechanical tension of the WG is already reduced. Usage of available wind energy is achieved too; specifically under low wind speeds. The whole system is used in electric vehicle application. In order to evaluation of the proposed system performormance, simulation is runned by MATLAB/Simulink. The result confirms its advantages.*
Keywords: *Brushless DC motor (BLDC), electric vehicle (EV), wind generator (WG), maximum power point tracking (MPPT)*

1. Introduction

Nowadays, renewable energy resources become important and interesting because of their advantages such as pollution-free and unlimited energy supplies. The wind power generation system (WPGS) is one of the most effective generation systems, developed to capture and change the form of energy from wind one into electricity. Most of WPGSs have considerable cost–performance ratio and are attractive to investment. Due to higher reliability and more appropriate size of the small-scale WPGS, it is more suitable than the large-scale ones for urban environment. Recent research studies about small wind turbine global market, made by the American Wind Energy Association in 2007 [1], have found that the micro-scale WPGS is a subset of the small-scale ones and a WPGS with capacity of less than 1kW is applicable in electric vehicle drive application. Typically, wind turbine with fixed pitch angle, permanent-magnet (PM) generator, rectifier, dc converter, battery module, and a dc load are different parts of a small size WPGS. In order to make them more efficient, using one of the maximum power point tracking (MPPT) control algorithms are more common. It regulates turbine rotor speed according to actual wind speeds. Basically, there are four different types of MPPT techniques, namely, the tip speed ratio (TSR) control, the optimal torque (OT) control [2], [3], the power mapping control [4], [5], and the perturbation and observation (P&O) searching control [6], [7].

Due to disadvantages of conventional electric motors such as dc brushed motors, single and three phase induction ones, attention to other type of motors has increased. One of them which has absorbed many interesting, is brushless DC motor (BLDCM).Some of its attractive features are high efficiency and energy saving, it can operate efficiently all over the speed range, more reliable than of brushed DC motors and more efficient than AC variable frequency motor on the rated frequency. Furthermore, comparing with conventional AC and DC motors, there is an improvement on driving mileage about 20% to 50% in the brushless mag-

Received on: 12.12.2012
Accepted on: 03.08.2013

net motor, they also expand battery life by 30%. In this paper a control system for driving a BLDCM which is used in electric vehicle, is developed based on its mathematical model. The proposed system is supplied by a wind-generator (WG) which is used maximum-power point tracking (MPPT) algorithm through a high efficiency buck-type dc/dc converter and control unit, running the MPPT function, whithout any need to optimal power characteristic of WG or an anemometer. Furthermore, WG also operates in variable speed. Thus, the system has higher reliability, lower complexity and cost, and less mechanical stress.

BLDCM with new power converter topology is proposed by Krishnan and Shiyoung [12]. Four switch three phase brushless motor in low cost commercial applications is proposed by Krishnan [13]. The mentioned literature does not cope with modeling and simulation problems of buck converter fed BLDCM drive. In this paper, the buck converter for using in BLDCM drive is proposed.

2. Electric Vehicle Driven Motor Analysis with Wind Turbine

Although battery technology has been developed, but yet constrains large-scale automotive application. Improving energy efficiency as well as driving course and proper usage of the battery with energy management are topics of electric vehicle research area. Two important items that develop the electric vehicle technology are as follows:

i) Electric motor driver, using of a suitable driver according to characteristic of the battery.

ii) Electric vehicle motor, because of battery constraints, electric vehicles is used chiefly for urban traffic; the main duration of the vehicle operation is in start, acceleration and braking working conditions. Therefore, the motor startup and acceleration performance, the efficiency in low-speed condition, braking and energy recovery ability, overload capability, electrical energy density and the reliability of electric vehicle motor are particularly important problems.

Based on the two points mentioned above, the driven-motor have an important effect on the electric vehicle performance, therefore, proper selection of the electric vehicles motor depends on not only to the battery discharge characteristics, but also relates to the vehicles operation characteristics too.

A new strategy for using renewable energy sources such as wind turbines is instilling them below the front bumper or on the car's roof as is shown in Fig.1. When the car moves along, it comes up against the air resistance. The resistance of the air mass hits turbine blades and leads to generate electricity. The produced energy is saved on the battery, and then used in the BLDC motor. So, for producing energy, less fuel is needed and decreases the cost.

3. Mathematical Model of BLDC

The schematic module and the control unit of BLDC motor and is shown in Fig. 2. The brushless DC motor is actually a permanent magnet AC motor whose torque-current characteristics act similar with a DC motor, but uses electronic brushless commutation system. BLDC is a modified PMSM with trapezoidal back-emf instead of sinusoidal [8]. It is important to know the rotor position in order to follow the proper energizing sequence [9]. In this system, Hall effect sensors is used to sense position of the rotor, namely Hall_A, Hall_B, and Hall_C, embedded into the stator with a lag of 120º from the earlier. The position of the rotor is determined using Hall sensors and related windings are excited. Since a BLDC motor is easy to control, it is the choice in many applications requiring precise control of speed [10], [11].

Based on motor model, the electromagnetic torque, T_{em} has a linear relationship with the armature current i_a i.e., $T_{em} = k_T \cdot i_a$, where k_T is the torque constant. The back- emf in a BLDC motor is linearly proportioned to the rotational mechanical speed and its direction is determined by Flemings right hand rule. Supposing that intensity of magnetic field is B, length of conductor on the edge of rotor is *l*, the number of conductors in the motor is Z rotor radius is *r* and rotor is rotating at an angular velocity of ω_r, then the speed of the conductor is given by:

Figure 1. Electric vehicle with wind turbine.

$$v_{el} = r.\omega_r \tag{1}$$

The emf e in that conductor is given by:

$$e = \omega_r Bl(Z/2) \tag{2}$$

The relationship between back-emf and angular velocity of rotor is:

$$e = K_\varphi \omega \tag{3}$$

Where, K_φ is the back-emf constant. In three phases BLDC model the sum of the phase currents has to be zero, i.e.

$$i_a + i_b + i_c = 0 \tag{4}$$

The following three phase equations are used to model the two pole three phase BLDC motor:

$$\begin{bmatrix} v_a \\ v_b \\ v_c \end{bmatrix} = \begin{bmatrix} R_a & 0 & 0 \\ 0 & R_b & 0 \\ 0 & 0 & R_c \end{bmatrix} \begin{bmatrix} i_a \\ i_b \\ i_c \end{bmatrix} + \frac{d}{dt} \begin{bmatrix} L_a & L_{ba} & L_{ca} \\ L_{ab} & L_b & L_{cb} \\ L_{ac} & L_{bc} & L_c \end{bmatrix} \begin{bmatrix} i_a \\ i_b \\ i_c \end{bmatrix} + \begin{bmatrix} e_a \\ e_b \\ e_c \end{bmatrix} \tag{5}$$

The rotor field is induced by the permanent magnet, embedded in the shape of an arc, inductances of each phase be without dependence on the rotor position, hence:

$$L_a = L_b = L_c = L_p \tag{6}$$

$$L_{ab} = L_{ba} = L_{bc} = L_{cb} = L_{ca} = L_{ac} = M \tag{7}$$

Eequation (5) is simplified as follows:

$$\begin{bmatrix} v_a \\ v_b \\ v_c \end{bmatrix} = \begin{bmatrix} R_a & 0 & 0 \\ 0 & R_b & 0 \\ 0 & 0 & R_c \end{bmatrix} \begin{bmatrix} i_a \\ i_b \\ i_c \end{bmatrix} + \begin{bmatrix} L_p & M & M \\ M & L_p & M \\ M & M & L_p \end{bmatrix} \frac{d}{dt} \begin{bmatrix} i_a \\ i_b \\ i_c \end{bmatrix} + \begin{bmatrix} e_a \\ e_b \\ e_c \end{bmatrix} \tag{8}$$

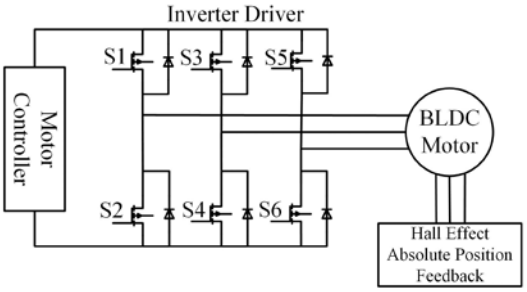

Figure 2. The schematic module of BLDC motor.

Reordering the earlier equations leads to equation (9):

$$\begin{bmatrix} v_a \\ v_b \\ v_c \end{bmatrix} = \begin{bmatrix} R_a & 0 & 0 \\ 0 & R_b & 0 \\ 0 & 0 & R_c \end{bmatrix} \begin{bmatrix} i_a \\ i_b \\ i_c \end{bmatrix} + \begin{bmatrix} L_p - M & 0 & 0 \\ 0 & L_p - M & 0 \\ 0 & 0 & L_p - M \end{bmatrix} \frac{d}{dt} \begin{bmatrix} i_a \\ i_b \\ i_c \end{bmatrix} + \begin{bmatrix} e_a \\ e_b \\ e_c \end{bmatrix} \tag{9}$$

4. WG Control Strategy

In this paper, in order to execute maximum power-point-tracking (MPPT) control of WG, another approach is described. Fig.3 represents the block diagram of the proposed system model. In this MPPT process, output power is monitored by using the WG output voltage and current measurements. The dc/dc converter duty cycle is directly adjusted according to the result of comparison between successive WG-output power values. Thus, knowledge of the WG power versus the rotor speed or wind velocity characteristic is not required. WG is protected from over-speeding by using a resistive dummy load. The WG wind and rotor-speed ratings or the dc/dc converter power rating do not restrict the proposed MPPT method applications. Although the proposed method has been modeled for an application like charging a battery with a dc/dc converter, but it is also able to use in electric vehicle drive application.

4.1. WG Characteristics

The power derived from wind by the WG turbine blades, P_m, depends on the blade shape, the pitch angle, and the radius and the rotor speed of rotation as follows:

$$P_m = 0.5\pi\rho C_p(\lambda,\beta)R^2V^3 \quad (10)$$

Where ρ is the air density (typically 1.25 kg/ m3), β is the pitch angle (in degrees), R is the blade radius (in meters), V is the wind speed (in m/s) and $C_p(\lambda,\beta)$ is the wind-turbine power coefficient that is a function of TSR λ.

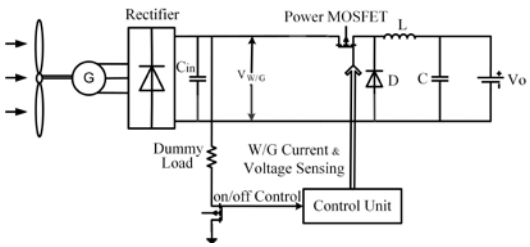

Figure 3. Block diagram of the proposed system (motor controller).

The termis λ the tip-speed ratio, defined as:

$$\lambda = \frac{\Omega R}{V} \quad (11)$$

Where Ω is the WG rotor speed of rotation (rad/s). If the generator efficiency is η_G, so the total generated power by the WG, P, is expressed as:

$$P = \eta_G P_m \quad (12)$$

When the blades pitch angle is equal with zero, the WG power coefficient is maximized for optimum value of tip-speed ratio λ_{opt}. In the characteristic curves of WG output power for various wind speeds there is a specific point where the output power is maximum. Therefore, maximum power is obtained continuously from the wind (MPPT control) by controlling the load of WG in variable-speed operation. TSR value is constant through all maximum power points (MPPs). This leads to linear relationship between the rotational speed of WG and the wind velocity as follows:

$$\Omega_n = \lambda_{opt}\frac{V_n}{R} \quad (13)$$

Where Ω_n is the optimal rotational speed of WG at a wind velocity V_n. operation of wind turbines provides 10% to 15% higher output energy, lower mechanical stress and less power fluctuation [14]. The disadvantage of the variable-speed operation is requirement of a power stabilizer as the WG dummy load. However, the development of power electronics leads to reduce the power-converter cost and also augment its reliability, while the higher cost can be compensated by the energy production gain.

Fig.4 shows characteristic curves of the WG torque, including the interconnected wind-turbine/ generator system, for various output voltage levels of generator under different wind velocities. The generator is designed to act in the almost linear region, according to the straight part of the generator torque curves in Fig. 4, under any wind-speed condition. Intersection point of the generator torque curve and the wind-turbine torque curve is the WG operating point. During the MPPT process, applying different changes in the WG load leads to various generator output voltage levels; thus, the generator torque is adjusted in order to act at the target torque under various wind speed. The target-torque line related to the optimal-power production line is shown in Fig. 4, where the energy captured from the WG system is maximum value.

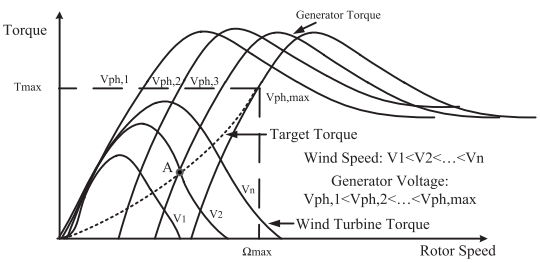

Figure 4. Torque-speed characteristics of the wind turbine and the generator.

4.2. MPPT Algorithm

As mentioned in Section I, in the MPPT process of the proposed system, the dc/dc converter duty cycle is directly adjusted by the result of the comparison between WG-output-power measurements. On the contrary of the wind speed that varies highly with

time, the power captured by the WG varies relatively slowly. This is due to the slow dynamic response of the interconnected wind-turbine/generator system. Thus, the steepest ascent method is used to remove the problem of extracting the maximum output power of the WG with controlling the converter duty cycle. This method conforms to the following control law:

$$D_k = D_{k-1} + C_1 \frac{\Delta P_{k-1}}{\Delta D_{k-1}} \quad (14)$$

Where D_k and D_{k-1} are the duty-cycle values at iterations k and $k-1$, respectively ($0 < D_k < 1$); $\Delta P_{k-1} / \Delta D_{k-1}$ is the WG power gradient at step $k-1$; and C_1 is the step change.

In order to show the feasibility of the proposed method and its convergence to the WG MPP under each wind-speed condition, it is sufficient to confirm that the function P(D), that depends on the WG power P and the dc/dc converter duty cycle D, has a single extreme point coincides in the WG MPPs, which are depicted in Fig. 4. With regard to the WG power characteristic curves are depicted in Fig. 4, it is obvious that at the points of maximum power production,

$$\frac{dP}{d\Omega} = 0 \quad (15)$$

Where Ω is the WG rotor speed.

Also by applying the chain rule, the above equation is written as:

$$\frac{dP}{d\Omega} = \frac{dP}{dD} \cdot \frac{dD}{dV_{WG}} \cdot \frac{dV_{WG}}{d\Omega_e} \cdot \frac{d\Omega_e}{d\Omega} = 0 \quad (16)$$

Where V_{WG} is the rectifier output voltage level and Ω_e is the generator-phase-voltage angular speed.

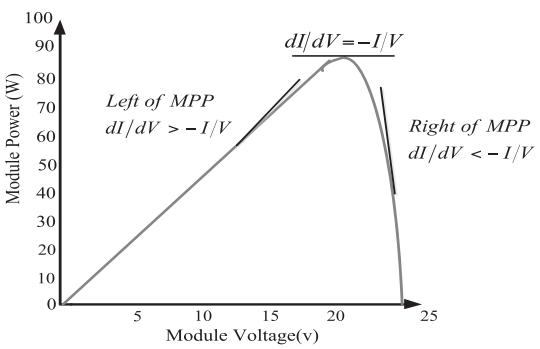

Figure 5. MPP tracking process.

In the case of a buck-type dc/dc converter, the output (battery) voltage level is related to input voltage level and the duty ratio is defined as follows:

$$D = \frac{V_o}{V_{WG}} \rightarrow \frac{dD}{dV_{WG}} = -\frac{V_o}{V^2_{WG}} \neq 0 \quad (17)$$

Where V_o is the battery voltage level. The relationship between wind-turbine rotor speed and generator speed is expressed as follows:

$$\Omega_e = p \cdot \Omega \rightarrow \frac{d\Omega_e}{d\Omega} = p > 0 \quad (18)$$

Where p is the number of pole pairs in generator. The rectifier output voltage V_{WG} is proportional to the generator phase voltage V_{ph}. According to Fig. 5:

$$\frac{dV_{ph}}{d\Omega e} > 0 \quad (19)$$

$$\frac{dV_{WG}}{d\Omega_e} > 0 \quad (20)$$

With regard to (16)–(20), it leads to:

$$\frac{dP}{d\Omega} = 0 \Leftrightarrow \frac{dP}{dD} = 0 \quad (21)$$

Therefore, it is approved that the function *P(D)* has a single extreme point. This point also coincides in the WG MPP, and adjusting the duty cycle of dc/dc converter duty-cycle under the control law of (15) leads to convergence to the WG MPP under various wind-speed states. The maximizing process of power is shown in Fig. 5. Owing to the duty-cycle adjustment follows the direction of dP/dD, in the right side of the WG characteristic curve, the duty-cycle value is augmented. The increased duty ratio in Buck converter will result in decreasing WG-rotor-speed and increasing power. Duty-cycle growth will be continued until the MPP is achieved.

Similarly when the starting point of process is situated in the left side of characteristic curve, following the direction of dP/dD results in duty-cycle becomes smaller and the speed of WG rotor higher, eventually convergence is happened at the MPP.

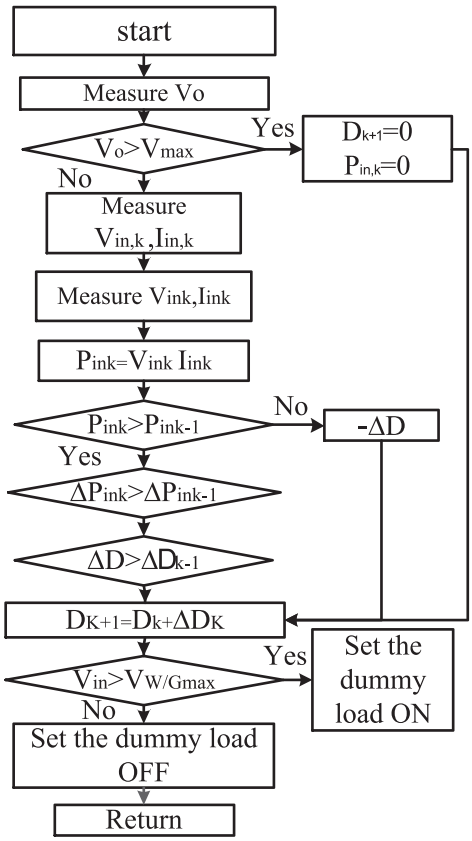

Figure 6. MPPT process algorithm

The flowchart algorithm of the control system is illustrated in Fig. 6. The battery voltage is observed and when it gets to level higher than threshold value, charging status is finished and the MPPT operation is stopped in order to protect the battery stack from being overcharged. In order to determine the sign of the duty-cycle change ΔD, the WG output power at the current iteration is computed and compared to the WG output power at the previous one of the algorithm. Based on the comparison result, the sign of ΔD will be reversed or remain unchanged and subsequently the variation of PWM output duty cycle is applied properly, according to the control law described by (15).

After adjusting the duty-cycle, the voltage level of WG must be measured. Based on the result, two modes can be happened, When it is below the maximum predefined value, the dummy load is separated from the circuit. On the contrary, when it is upper than the maximum predefined value, this load is connected to the dc/dc converter input to prevent the WG from over speeding. The hysteresis limits are set by the maximum and minimum predefined value. This is necessary to stop the dummy load from continuing its on/off state.

5. Simulation Results

Parameters of BLDC motor that is used for simulation are listed in table.1. In order to evaluate the operation of proposed system, the wind velocity variation is shown in Fig. 7. The WG output power and the rotor speed are shown in Fig. 8. It is apparent that the WG output power profile imitates the wind speed changes. It can be seen from Fig. 8 that due to the improved dynamic response the power comes rapidly near to its final value. It results to less energy consumption. Also by implementing the proposed system, more wind energy can be obtained in the higher wind speed variation. The generator current wave form of the proposed system is illustrated in Fig. 9.

Table 1. Parameters of BLDC Motor.

Items	Specification
Inverter	MOSFET
Stator resistance	Bridge
Stator inductance	Rs=2.95 Ω
Flux induced by	Ls=6e-3 H
magnets	0.183 W
Back emf flat area	120 degrees
Inertia	0.2e-3
Friction factor	1e-3
Pole pairs	4

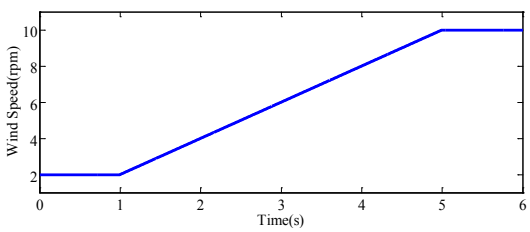

Figure 7. Wind speed versus time.

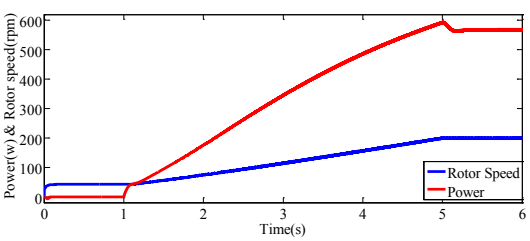

Figure 8. Output and Rotor speed, versus time.

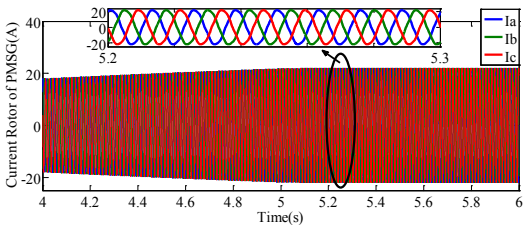

Figure 9. Generator current .

Pi-filter is used for filtering the buck converter output. The output of the pi-filter is implemented to the three phase inverter and the BLDC is supplied by three phase inverter voltages. Pulse width is 33% and output voltage level of Buck converter is 24 V. Voltage wave forms of the three phase inverter are shown in Fig. 10. The voltages are shifted by 120º. Three phase currents are given by the motor are shown in Fig. 11. The back-emfs are prepared for applying to the three phases of motor are shown in Fig. 12. Fig. 13 represents speed of rotor. As it can be seen, just before 1s motor reaches almost its final value due to fast dynamic response of motor and proper effect of the control system.

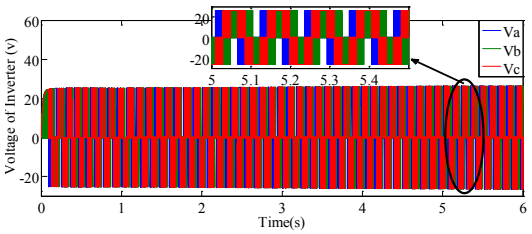

Figure 10. Voltages of inverter.

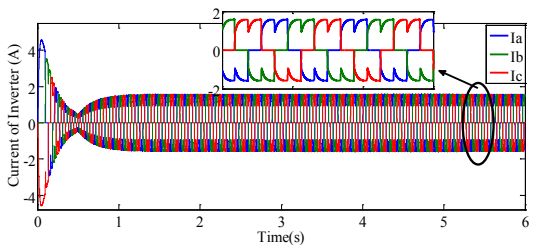

Figure 11. Output currents of inverter.

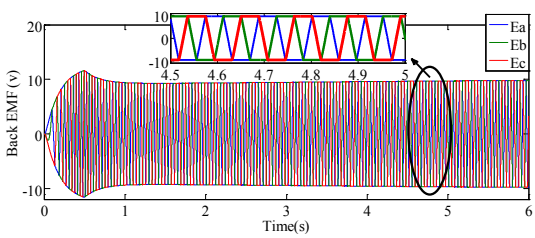

Figure 12. Back EMF waveforms

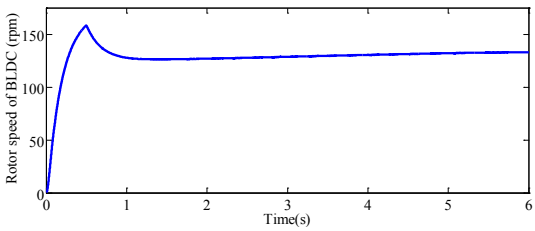

Figure 13. Rotor speed of BLDC.

6. Conclusions

A control system which is appropriate for driving a BLDCM in electric vehicle application has been presented in this paper by using its mathematical model. Because the motor is supplied by the wind generator, a MPPT technique was presented to increase the efficiency and improve operation of the system. It is done by using a buck type dc/dc converter which is high efficiency, and MPPT managing control unit. Performance of the proposed system and its advantages are analyzed by MATLAB/Simulink. The results verify operation of the proposed system such as improving the dynamic response, although no need to anemometer. Furthermore, WG acts in variable speed mode, whereas mechanical stress and also power fluctuation are reduced. Moreover, application of the proposed MPPT method is not restricted by the capacity of WG, rotor-speed or power of dc/dc converter. Buck converter is used to decrease the input voltage to required value.

7. References

[1] AWEA. (2007, Jul.). AWEA small wind turbine global market study 2007, in *The American Wind Energy Association Small Wind Systems* [Online]. Available: http://www.awea.org/smallwind/

[2] M. Knight and G. E. Peters, "Simple wind energy controller for an expanded operation range," *IEEE Trans. Energy Convers.*, vol. 20, no. 2, pp. 459–466, Jun. 2008.

[3] S.Morimoto, H. Nakayama,M. Sanada, andY. Takeda, "Sensorless output maximization control for variable-speed wind generation system using IPMSG," *IEEE Trans. Ind. Appl.*, vol. 41, no. 1, pp. 60–67, Jan./Feb. 2005.

[4] K. Tan and S. Islam, "Optimum control strategies in energy conversion of PMSG wind turbine system without mechanical sensors," *IEEE Trans. Energy Convers.*, vol. 19, no. 2, pp. 392–399, Jun. 2004.
[5] F. Valenciaga and P. F. Puleston, "Supervisor control for a stand-alone hybrid generation system using wind and photovoltaic energy," *IEEE Trans. Energy Convers.*, vol. 20, no. 2, pp. 398–405, Jun. 2005.
[6] E. Koutroulis and K. Kalaitzakis, "Design of a maximum power tracking system for wind-energy-conversion applications," *IEEE Trans. Ind. Electron.*, vol. 53, no. 2, pp. 486–494, Apr. 2006.
[7] R. Datta and V. T Ranganathan, "A method of tracking the peak power points for a variable speed wind energy conversion system," *IEEE Trans. Energy Convers.*, vol. 18, no. 1, pp. 163–168, Mar. 2009.
[8] Luk, P.C.K. and C.K. Lee, 1994. Efficient modeling for a brushless DC motor Drive. 20th International conference on Industrial Electronics, Control and Instrumentation, IECON'94, 1: 188-191.
[9] A. Sathyan, N. Milivojevic, Y. J. Lee, M. Krishnamurthy, and A. Emadi,"An FPGA-based novel digital PWM control scheme for BLDC motor drives," *IEEE Trans. Ind. Electron.*, vol. 56, no. 8, pp. 3040–3049, Aug. 2009.
[10] Atef, S.O. and Al-Mashakbeh, 2009. Proportional Integral and derivative control of brushless DC motor. Eur. J. Sci. Res., 35(2): 198-203.
[11] Byoung-Kuk, L., K. Tae-Hyung and J. Mehrdad Ehsani, 2001. On the feasibility of four-switch three phase BLDC motor drives for low cost commercial applications topology and control. IEEE Tran. Power Electron., APEC, 18(1): 428-433.
[12] Krishnan, R. and L. Shiyoung, 1997. PM brushless DC motor drive with a new power-converter topology. IEEE Tran. Indus. Appl., 33(4): 973-982.
[13] Krishnan, R., 2003. A Text Book on Electric Motor Drives, Modelling, Analysis and Control. Prentice Hall of India Pvt Ltd., New Delhi.
[14] Q. Wang and L.-C. Chang, "An intelligent maximum power extraction algorithm for inverter-based variable speed wind turbine systems," *IEEE Trans. Power Electron.*, vol. 19, no. 5, pp. 1242–1249, Sep. 2004.

Saeed Masoumi Kazraji was born in Tehran, Iran in 1989. He received the B.Sc. degree from the Sbzevar University of Tarbiat Moallem, Mashhad, Iran in 2011 and the M.Sc. degree from University of Tabriz, Tabriz, Iran in 2013. both in Electrical Power Engineering. He is currently pursuing the Ph.D. University of Tabriz. Degree in electrical engineering (machine and electric drives). His research interests include drive and motion control of electric machines, linear and rotary machine design, renewable energy in electric vehicle drive application, and power electronic converters.

Saheb Khanabdal was born in Gorgan, Iran, in 1989. He received the B.S. degree from Khaje Nasir Toosi University of Technology (KNTU),Tehran, Iran, in 2011 and the M.S degree from University of Tabriz, Tabriz, Iran in 2013, both in electrical engineering. He is currently working toward the Ph.D. degree with the Department of Electrical Engineering, University of Shahrood, Shahrood, Iran.
His main research interests include electrical machines, electrical vehicles, renewable energy and power electronics.

Mohammad Hosein Holakooie was born in Iran. He received the B.Sc. and M.Sc. degrees in electrical engineering from Guilan and Tabriz University, respectively. He is currently working toward the Ph.D. degree in electrical engineering at Zanjan University, Zanjan, Iran. His research interests include Electric drive, power electronics and Linear actuator.

Mohammad Bagher Bannae Sharifian (1965) studied Electrical Power Engineering at the University of Tabriz, Tabriz, Iran. He received the B.Sc. and M.Sc. degrees in 1989 and 1992 respectively from University of Tabriz. In 1992 he joined the Electrical Engineering Department of the University of Tabriz as a lecturer. He received the Ph.D. degree in Electrical Engineering from the same University in 2000. In 2000 he rejoined the Electrical Power Department of Faculty of Electrical and Computer Engineering of the same university as Assistant Professor. He is currently Professor of the mentioned Department. His research interests are in the areas of design, modeling and analysis of electrical machines, transformers, liner electric motors, and electric and hybrid electric vehicle drives.